

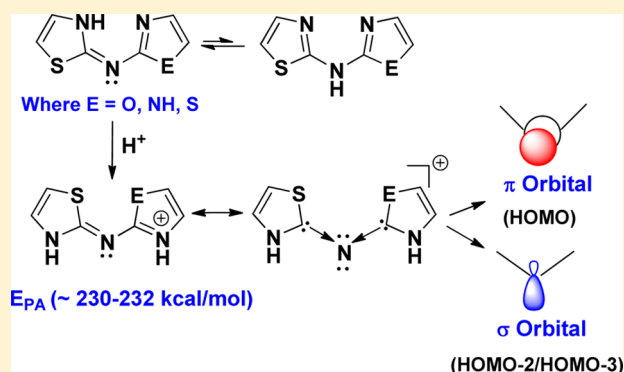
Possibility of the Existence of Donor–Acceptor Interactions in Bis(azole)amines: An Electronic Structure Analysis

Sonam Bhatia and Prasad V. Bharatam*

Department of Medicinal Chemistry, National Institute of Pharmaceutical Education and Research (NIPER), Sector 67, S. A. S. Nagar, Punjab 160 062, India

Supporting Information

ABSTRACT: Donor-stabilized divalent N(I) systems have recently gained attention in the field of organic chemistry. Existence of low-valent nitrogen(I) species with moderate nucleophilicities in several pharmacophoric functionalities is prompting extensive exploration in this field. Quantum chemical analysis on the imidazole, oxazole, and thiazole derivatives of thiazole-2-amine indicated that these species preferably exist in the iminic state. Electronic structure analysis of these systems suggested the existence of hidden divalent N(I) character in a neutral state ($L \rightarrow N-R$) and the explicit divalent N(I) character ($L \rightarrow N \leftarrow L$)⁺ in the protonated state. The strength of $L \rightarrow N$ interaction in these systems was analyzed, and the variations in the nucleophilicity trend at the coordinating nitrogen center were rationalized by estimating the electronic (TEP (Tolman electronic parameter) and MESP minimum (V_{\min})) as well as steric parameters (r -repulsiveness and ΔH elimination of CO group, in $L \rightarrow Ni(CO)_3$) of the coordinating ligands L. The importance of energetically preferred ionic and tautomeric representations of thiazol-2-amine derivatives in iminic and aminic forms was also demonstrated by carrying out comparative docking analysis with the enzyme lymphocyte-specific kinase (Lck).



1. INTRODUCTION

Recent reports on the existence of an atypical bonding situation in the ($L \rightarrow C \leftarrow L$) systems (called carbenes) with carbon in the C(0) state^{1–13} are challenging the traditional notions regarding the bonding states of carbon, which is well-known to exist in C(IV) and C(II) states. Such C(0) compounds have gone through intense experimental and theoretical investigations due to their strong electron-rich character.^{1–13} The pioneering work in this field therefore resulted in the establishment of unusual bonds like ($L \rightarrow E$) in many compounds with main group element E (where E = C,^{1–15,33} Si,^{14–18} Ge,^{15,17,19} Sn,^{15,17} Pb,¹⁵ N,^{20,21} N⁺,^{22–29,35} P,^{30,31} P⁺,^{32,33} B,^{34–36} As,^{37,38} etc.) and L (electron-donating groups: PR₃,^{33,21} diamino carbene,²⁷ N-heterocyclic carbenes (NHC),^{35,23,25,27,28} and cyclopropenium carbene,^{20,29} etc.). Electronic structure studies were carried out, various compounds were designed, a few compounds were newly synthesized, and a number of already existing compounds were analyzed with reference to this new perspective.^{1–38} Similarly, there are several studies reporting novel bonding. Among these, the compounds with divalent N(I) character (I–IV, Scheme 1) are of special interest because many medicinally important species carry the newly identified electronic interaction ($L \rightarrow N$).^{24–28} In our previous studies, we have already discussed the existence of this unusual bonding environment in drugs like metformin (antidiabetic),²⁵

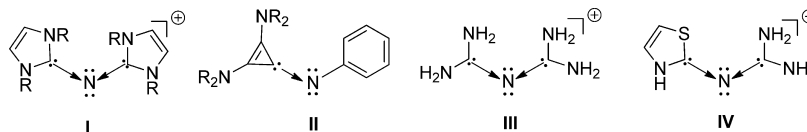
famotidine (antiulcerative),²⁷ ebrotidine (antiulcerative),²⁷ and cycloguanil (antimalarial).²⁵ There was a suggestion in the literature to restrain from using such $L \rightarrow E$ coordination bond descriptions,³⁹ and there is also suggestion to increase exploration of systems with such $L \rightarrow E$ coordination bonding situations.⁴⁰ In addition, there is an ongoing intense scientific exploration on the novel chemical bonding descriptions because most of the current bond definitions are based on diatomic models.⁴¹ The current paper contributes to the ongoing discussion on the chemical bonding.^{42–46}

Frenking and co-workers³⁵ have reported the electronic properties of cationic nitrogen complexes ($L \rightarrow N \leftarrow L$)⁺ and therefore established them as isoelectronic homologues of ($L \rightarrow C \leftarrow L$) systems. Alcarazo and co-workers synthesized divalent N(I) based ligands and studied their coordination behavior with transition metals.²⁰ Continuing the work, this group synthesized and characterized several carbene-stabilized N-centered cations (including ($L \rightarrow N \leftarrow L$)⁺ species) with cyclopropenium ligands.²⁹ The donor–acceptor bonding in these complexes is quite intriguing; these results prompted us to launch an extensive search for systems with $L \rightarrow N$ bonds among the medicinally important chemical species. The electronic structure of the compounds containing (thiazol-2-

Received: December 26, 2013

Published: May 9, 2014



Scheme 1. General Structures of a Few ($L \rightarrow N-R$) and ($L \rightarrow N \leftarrow L$)⁺ Systems

ylidene) \rightarrow N interaction (IV) were reported in the previous work on thiazolylguanidine class of compounds, in which the thiazol-2-ylidene group has been shown to carry electron-donating capacity.²⁷ This can be justified because the thiazol-2-ylidene ring has carbene-like character (NHC) and thus shows strong nucleophilicity.⁴⁷ To further explore the nature of (thiazol-2-ylidene) \rightarrow N interaction and to compare the electron donating capacity of thiazole vs imidazole vs oxazole rings and to estimate an electron localization at the coordinating nitrogen during the $L \rightarrow N$ interactions, quantum chemical calculations were performed on thiazole, imidazole, and oxazole substituted bis(azole)amines (TT, TI and TO, Figure 1).

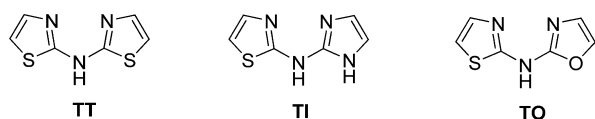


Figure 1. Thiazol-2-amine-derived analogues.

Derivatives of TT, TI, and TO have been known in medicinal chemistry for many years and carry a special class of pharmacophoric functionality, which is responsible for important therapeutic activities such as anticancer,^{48–51} antiinflammatory,^{52,53} and antimicrobial^{54,55} and also demonstrates gastro protective action⁵⁶ (2D structures of medicinally relevant bis(azole)amine derivatives are provided in Figure S1, Supporting Information). The X-ray crystal structures of TT, TI, and TO analogues indicated that these systems should be considered as derivatives of thiazol-2-imine rather than thiazol-2-amine.^{57,58} However, in the organic and medicinal chemistry literature the analogues of TT, TI, and TO classes of compounds are generally considered as thiazol-2-amine derivatives,^{48,49,55,56,59} which is a misleading perception. Therefore, establishing the electronic structure and identifying predominant state for these intriguing compounds is a subject of thorough theoretical studies. In the parent species 2-aminothiazole, amino–imino tautomerism is reported, and the amino form predominates in gas as well as solution phase by ~ 8 kcal/mol.⁶⁰ This value is rather small; upon substitution at the nitrogen center, iminic tautomers becomes almost isoenergetic to that of aminic tautomers and studies on *N*-(pyridine-2-yl)thiazol-2-amine have supported this argument.²⁸ This prompted us to take up thorough conformational analysis of the title compounds.

Thiazolamine derivatives (TT, TI, and TO) are highly basic as they readily form salts of acetate, trifluoroacetate, 1,1,1-trifluoromethanesulfonate, perchlorate, picrate, and hydrochloride.⁶¹ In principle, protonation can occur either at the ring nitrogen or central nitrogen; hence, it is important to establish the preferred protonation center and to explore the electronic character of the resultant species. Quantum chemical calculations using DFT (density functional theory) method have been performed to explore the same. Further, the effect of N-, S-, and O-based heteroazol-2-ylidenes on the donor–

acceptor strength ($L \rightarrow N$) in the divalent N(I) system was also quantified as these trends are not rationalized earlier. These topics are addressed in this paper in four different sections: (i) Establishing Preferred Tautomeric State (Imine vs Amine), (ii) Protonation Studies, (iii) Evaluation of Divalent N(I) Character in the Protonated State, and (iv) Molecular Docking Analysis.

2. COMPUTATIONAL DETAILS

Geometry optimizations on all possible isomers of TT, TI, and TO were performed using density functional (DFT)⁶² (B3LYP^{63,64} and ω B97X-D⁶⁵) calculations with the 6-311+G(d,p) split-valence triple- ζ basis set as implemented in the GAUSSIAN 09 package.⁶⁶ Frequencies were also computed analytically at the same basis set for all optimized species to characterize each stationary point as a minimum or a transition state and to estimate the zero-point vibrational energies (ZPE). The scaled ZPE (at 298.15 K) values were used for the calculations.⁶⁷ For considering the effect of dispersion on the relative stabilities of various isomers of TT, TI, and TO systems, optimization along with the frequency calculations was carried out for each isomer at ω B97X-D/6-311+G(d,p) level of approximation. Calculations were repeated at the B3LYP/6-311+G(d,p) level of theory using the CPCM (continuum polarizable conductor model)⁶⁸ solvent analysis method in the aqueous medium (implicit) for studying the effect of solvent on the relative energy trends of isomers under investigation. In addition to this, the trends in relative energy for different isomers were also calculated in the presence of an explicit water molecule under the gas phase and implicit solvation model (CPCM). The geometry optimization for all the protonated isomers of TT1, TI1, and TO1 was carried at the B3LYP/6-311+G(d,p) level in order to find the global minimum forms of protonated species. The partial atomic charges were estimated by the natural bond orbital (NBO)⁶⁹ method using the internal module of Gaussian 09 at the MP2(full)/6-311+G(d,p) level of theory. Intramolecular H-bonding and electrostatic interactions were computed by performing AIM (Atoms In Molecules) calculations using the AIM2000 software package.⁷⁰ ELF (Electron Localization Function)⁷¹ calculations were done on some important species to estimate the extent of electron density localization. The delocalization was measured by estimating the Bird index (BI) using Multiwfn version 3.2.⁷² Absolute proton affinity values (APA)^{73,74} for ($L \rightarrow N-R$) (neutral) and ($L \rightarrow N \leftarrow L$)⁺ (protonated) divalent N(I) systems were estimated at B3LYP level with the 6-311+G(d,p) basis set. To study the effect of N-, S-, and O-based heteroazol-2-ylidenes on the coordinating behavior of ($L \rightarrow N \leftarrow L$)⁺ divalent N(I) systems, complex dissociation energies (D_e) of TTP1, TIP1, and TOP1 systems with various Lewis acids (BH₃, AlCl₃, and AuCl) were also estimated, the complexes of AuCl were optimized with mixed basis set 6-311+G(d,p) plus def2-TZVPP⁷⁵ where Au is treated with the def2-TZVPP basis set with the associated effective core potential (ECP), while the rest of the molecule is optimized using the 6-311+G(d,p) basis set. Further, to analyze the effect of dielectric constant of solvents on the coordinating strength of divalent N(I) systems, the calculations were carried out in four different solvents viz. dichloromethane, tetrahydrofuran, ethanol, and water with default dielectric constant values as defined in Gaussian 09. The ligand-donating capacity of N-, S-, and O-based heteroazol-2-ylidenes were estimated using TEP (Tolman electronic parameter), which is calculated by performing complexation studies of ligand with Ni(CO)₃.⁷⁶ The mixed basis set approach as stated for AuCl complexes was also used here. All optimized geometries were verified to have all real harmonic frequencies by frequency calculations, which

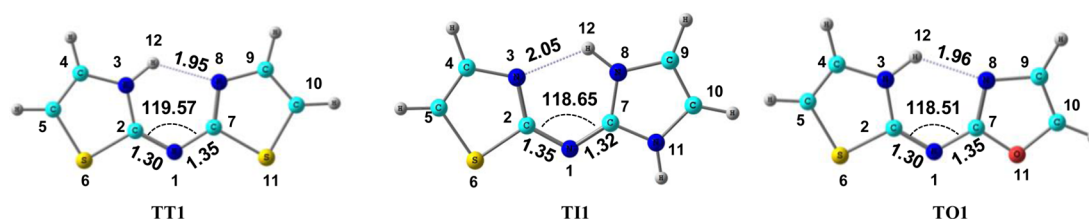


Figure 2. 3D-optimized geometries of stable isomers of TT, TI, and TO species. Bond lengths and intramolecular hydrogen bond distances are given in angstroms, and angles are given in degrees.

Table 1. Relative Gibbs Free Energies (kcal/mol) of All Possible Isomers of TT, TI, and TO Systems Calculated Using Different Quantum Chemical Methods in the Gas and Implicit Solvent Phase at the 6-311+G(d,p) Basis Set

isomers ^a	description wrt global minimum	gas phase		solvent phase	explicit (gas)	explicit + implicit (CPCM)	tautomer
		B3LYP	ω B97X-D	B3LYP ^b	B3LYP ^c	B3LYP ^d	
bis(thiazol-2-yl)amine							
TT1	global minimum	0.0	0.0	0.0	0.0	0.0	imine
TT2	1,3-H shift followed by N1–C2 rotation	1.9	1.4	1.3	–1.0	1.9	amine
TT3	N1–C2 rotation	2.5	3.0	0.5	–0.7	1.3	imine
TT4	1,3-H shift followed by N1–C2 and N1–C7 rotation	3.0	2.7	3.2	1.8	4.3	amine
TT5	N1–C2 and N1–C7 rotation	7.7	8.7	3.4			imine
TT6	1,3-H shift	7.8	7.4	4.9			amine
TT7	N1–C7 rotation	10.1	<i>e</i>	6.0			imine
N-(imidazol-2-yl)thiazol-2-amine							
TI1	global minimum	0.0	0.0	0.0	0.0	0.0	imine
TI2	1,5-H shift	0.3	0.3	1.4	1.9	1.7	imine
TI3	1,3-H shift	0.7	–0.1	1.5	0.5	1.2	amine
TI4	1,5-H shift followed N1–C2 rotation	3.9	4.6	2.4	6.5	3.1	imine
TI5	1,3-H shift followed by N1–C2 rotation	5.2	4.6	3.2			amine
TI6	1,3-H shift followed by N1–C2 and N1–C7 rotation	5.8	5.5	5.7			amine
TI7	N1–C2 rotation	9.6	10.5	5.5			imine
TI8	1,5-H shift followed by N1–C2 and N1–C7 rotation	11.5	<i>f</i>	6.7			imine
TI9	1,3-H shift followed by N1–C7 rotation	13.3	12.9	8.1			amine
N-(oxazol-2-yl)thiazol-2-amine							
TO1	global minimum	0.0	0.0	0.0	0.0	0.0	imine
TO2	1,3-H shift followed by N1–C2 rotation	1.6	1.1	2.3	–0.1	2.9	amine
TO3	N1–C2 rotation	2.5	3.2	0.6	–0.4	1.5	imine
TO4	1,3-H shift followed by N1–C2 and N1–C7 rotation	2.7	2.3	3.4	1.7	4.3	amine
TO5	N1–C7 rotation	6.4	7.4	3.2			amine
TO6	1,3-H shift	6.7	8.2	5.9			amine
TO7	1,5-H shift followed by N1–C2 and N1–C7 rotation	8.8	10.2	4.3			imine

^a3D-optimized geometries for the rest of the isomers are provided in Figure S2 (a–c) of the Supporting Information. ^bImplicit solvent analysis carried out using the CPCM solvent model with water as a solvent. ^cExplicit solvent analysis was carried out using one explicit water molecule under consideration. ^dCombined explicit and implicit solvent analysis was carried out using one explicit water molecule under consideration. ^eDuring complete optimization, the structure is converted to **TT1**. ^fDuring complete optimization, the structure is converted to **TI4**.

also provided the ν_{CO} frequencies. The MESP minimum (V_{min})⁷⁷ values for different NHCs were also calculated by using wave functions generated using the same method which is used to optimize geometries.

The nucleophilicity index (N), for neutral system was estimated by using the formula reported recently by Domingo et al.,⁷⁸ $N = E_{\text{HOMO}(\text{Nu})} - E_{\text{HOMO}(\text{TCE})}$, where tetracyanoethylene (TCE) is chosen as the reference. For the protonated species, the nucleophilicity index (N) is calculated using the inverse of electrodonating power (ω^-), where $\omega^- = (I^2/2(I - A))$; I is energy of HOMO and A is energy of LUMO.^{79–81}

To demonstrate the importance of correct tautomeric representation of **TZA** (thiazol-2-amine) derivatives during molecular docking analysis, docking studies were performed with the Lck kinase (PDB ID: 1QPC) reported by Zhu et al.⁸² The protein preparation wizard of Schrodinger package maestro version 9.3.5 was used to prepare the structure of Lck.^{83,84} Structural derivatives of **TT** and **TI** which were tested against the Lck inhibition by the research group of Das et al.⁵⁰

were taken into consideration in this study. The ligands were optimized using OPLS 2005 force fields of LigPrep module.⁸⁵ To standardize the protocol, the preliminary docking study was carried out with the highly potent Lck inhibitor BMS-358233, which reproduced the experimentally reported binding interactions. This protocol was subsequently used for performing multiple ligand docking analysis.

3. RESULTS AND DISCUSSION

3.1. Establishing Preferred Tautomeric State (Imine vs Amine). Quantum chemical studies performed on 2-(thiazol-2-yl)guanidine indicated that an amine tautomeric form is more stable by only ~ 0.44 kcal/mol than the corresponding iminic tautomer at B3LYP/6-31+G(d) level.²⁷ Similarly, studies on *N*-(pyridine-2-yl)thiazol-2-amine indicated that the amine tautomer is more stable by ~ 2.3 kcal/mol at the B3LYP level of quantum chemical analysis.²⁸ In both cases, thiazolamine \rightleftharpoons

thiazolimine tautomerism is possible.^{27,28} Considering that the crystal structure data on **TT**, **TI**, **TO** prefer the thiazol-2-iminic state for these systems,^{57,58} tautomeric equilibrium is expected in the bis(azole)amine class of compounds also. The quantum chemical analysis addressing this issue is presented in this section.

The 3D structures for the most stable isomers of **TT**, **TI**, and **TO** are given in Figure 2, and the relative energies of all possible isomers are illustrated in Table 1. These lowest energy forms are stabilized due to the presence of strong intramolecular hydrogen bonds. Molecular graphs generated through AIM analysis showed the bond critical points along the path of intramolecular hydrogen bonds and the ring critical points due to the hydrogen bond assisted ring formation (Figure S3, Supporting Information). In **TT**, the thiazolimine \rightleftharpoons thiazolamine tautomeric energy difference is (~ 2.0 kcal/mol) in favor of iminic tautomer. In the case of **TI**, two possible iminic isomers are possible, imidazolimine (**TI1**) and thiazolimine (**TI2**); both are almost isoenergetic on the potential energy surface, with **TI1** being marginally more preferable, while in the case of **TO** the preference for thiazolimine tautomer is again noticeable. The relative energy profiles for all of the possible isomers were also reviewed under an implicit solvation model which suggested the predominance of iminic tautomers by 1.3, 1.5, and 2.3 kcal/mol over the corresponding low energy aminic tautomers in the systems under investigation.

The calculated geometric parameters of **TT1** and **TO1** isomers are comparable with the crystal structure reported for similar derivatives confirming the stability of iminic forms.^{57,58} The energy difference between **TT1** and **TT2** is very small; i.e., imine \rightleftharpoons amine tautomer differences are less in bis(thiazol-2-yl)amines. It is not possible to declare the preferred structures because the imine \rightleftharpoons amine interconversion may take place rapidly at room temperature. However, based on the energy values, iminic structure may be considered to be marginally more preferred, and a similar observation is noticeable in the isomers of **TI** and **TO** species.

To further analyze the stability of **TT1**, **TI1**, and **TO1** iminic isomers over aminic isomers on the potential energy surface, the barrier for 1,3-H shift, which proceeds via a four-membered transition state (**TS1**, **TS2**, **TS4**, Figure S4, Supporting Information), was calculated and found to be in the range of ~ 45 – 54 kcal/mol. Thus, 1,3-H shift is an energy-demanding shift and is not expected to take place as a unimolecular process at normal reaction conditions. On the other hand, the 1,5-H shift is found to be a highly facile shift in these species. This can be based on low energy barriers (4.7 and 5.5 kcal/mol) obtained for six-membered transition state (**TS3**, **TS5**, Figure S4, Supporting Information), which resulted in the formation of **TI2** and **TO7** isomeric species, which are also iminic in nature. Thus, from the above studies, it can be concluded that 1,5-H shift is thermally allowed, whereas 1,3-H shift is thermally forbidden on the reaction path indicating the stability of iminic isomers.

Inclusion of dispersion effects (ω B97X-D) in the definition of quantum chemical method did not disturb the stability of global minimum isomers of **TT1** and **TO1** on their corresponding potential energy surfaces. However, in the **TI** system the marginal reshuffling in the order of stability between **TI1** and **TI3** is observed, making the latter to be more stable by 0.1 kcal/mol. As this value is exceptionally small, we ignored this insignificant change by examining the stability of **TI1** in

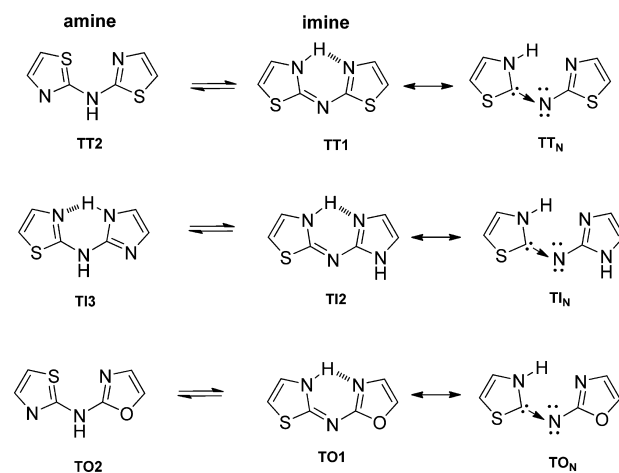
other models under consideration. The effect of microsolvation (both in explicit as well as combine explicit and implicit solvation model) on the relative stabilities of iminic vs aminic forms were also analyzed by keeping the explicit water molecule bound to the center nitrogen atom, and the results showed that the presence of explicit water in the presence of combine explicit and implicit solvation model enhances the thermodynamic stability of iminic–H₂O clusters over the corresponding aminic–H₂O clusters (Table 1 and Figure S5(a–c), Supporting Information), again supporting the predominance of iminic forms.

We also analyzed the stability of lower energy aminic structures **TT2**, **TI3**, and **TO2**, which are found to be planar as evident from their 3D structures (Figure S2(a–c), Supporting Information). The coplanarity between the two rings in these forms (**TT2** and **TO2**) can be attributed to the aromatic stabilization which is associated with the delocalization of electrons, along with the existence of through space S \cdots N interaction, which can be perceived from the molecular graphs generated by AIM analysis and show the presence of BCP along the path connecting S \cdots N as evident from Figure S3 (Supporting Information). A similar observation for intramolecular O \cdots P interaction is reported in σ^3 -phosphole systems.⁸⁶

Representing the structures of bis(thiazol-2-yl)amine (**TT**), *N*-(imidazol-2-yl)thiazol-2-amine (**TI**), and *N*-(oxazol-2-yl)thiazol-2-amine (**TO**) as given in Figure 1 is convenient but not appropriate, as these structures suffer from the lone pair (N) and lone pair (N) repulsions; the corresponding 3D structures **TT6**, **TI9** and **TO6** are high energy isomers (Table 1). The heterocyclic rings in **TT1**, **TI1**, **TI2**, and **TO1** may be treated as *N*-heterocyclic carbenes (heteroazol-2-ylidenes), and they can be represented as in **TT_N**, **TI_N**, and **TO_N** as shown in Scheme 2 because the heteroazol-2-ylidene groups are electron-donating moieties. Thus, **TT1**, **TI1**, **TI2**, and **TO1** are compounds with hidden divalent N(I) character as in **II**.²⁰

3.2. Protonation Studies. Compounds belonging to the bis(azole)amine class are known to form salts of multiple varieties, including dibasic salts.⁶¹ The partial atomic charges obtained from natural bond orbital analysis (NBO) indicated two possible sites for protonation in **TT**, **TI**, and **TO** systems. Figure 3 depicts the 3D structure of the most stable isomer of

Scheme 2. *N*-Substituted Thiazol-2-imines (**TT1**, **TI2**, and **TO1**), Their Structures in (L \rightarrow N–R) Representation, and Their Aminic Tautomers



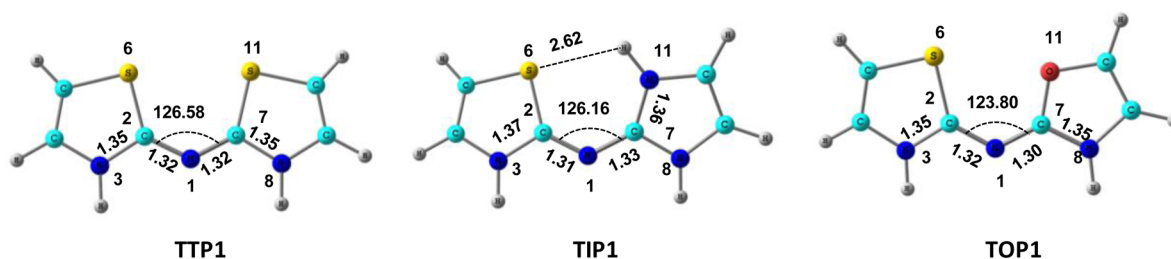


Figure 3. 3D-optimized geometries of protonated N-substituted thiazolimines. Important bond lengths are given in angstroms and angles in degrees.

protonated TT, TI, and TO systems. The proton affinity values ranging from ~ 230 to 232 kcal/mol for these systems are listed in Table 2, clearly indicating the highly basic nature of this class

Table 2. Relative Gibbs Free Energy and Proton Affinity (PA) of Various Isomers (kcal/mol)

conformer	site of protonation	description wrt global minimum	RE	PA	tautomer
TTP1	N8	global minimum	0.0	230.3	imine
TTP3	N1	1,3-H shift followed by N1-C2 and N1-C7 rotation	6.2	224.1	amine
TIP1	N3	global minimum	0.0	232.6	imine
TIP2	N1	1,3-H shift followed by N1-C2 rotation	5.4	227.2	amine
TOP1	N8	global minimum	0.0	230.2	imine
TOP4	N1	1,3-H shift followed by N1-C2 and N1-C7 rotation	8.1	222.1	amine

The relative energy values and 3D-optimized geometries for all the protonated isomers considered in this study are given in Table S1 and Figures S6–S8 of the Supporting Information.

of compounds. The potential energy surface of TTP, TIP, and TOP has been explored, and from this analysis, it is clearly evident that the structures with proton on the ring nitrogens (i.e., structure without proton on the central nitrogen) are more preferred.

Our previous studies on thiazolylguanidines,²⁷ biguanides,²⁵ guanylthioureas,²⁴ and pyridylthiazolamines²⁸ class of compounds indicated the presence of divalent N(I) character on central nitrogen in these functionalities. The electronic structures of TT1, TII, and TO1 undergo significant change upon protonation. Similarly, TTP1, TIP1, and TOP1 can be considered to carry divalent N(I) character at the central nitrogen. The rings in TTP1, TIP1, and TOP1 should be treated as thiazol-2-ylidene, imidazol-2-ylidene, and oxazol-2-ylidene, which carry carbene-like character, donating electron density to the central nitrogen through coordinate bond. This unusual bonding character ($L \rightarrow N \leftarrow L$)⁺ is explored in detail in these cationic nitrogen species, for which results are presented in the next section.

3.3. Evaluation of Divalent N(I) Character in the Protonated State. Patel et al.²³ reported the divalent N(I) character of the NHC coordinated nitrogen species (I). The central nitrogen in I (R = H) ($(L \rightarrow N \leftarrow L)^+$) carries an excess partial negative charge, and it increases with an increase in the electron-donating capacity of L.^{23,25} This excess electronic charge is manifested in the form of two lone pairs, which can be realized from the molecular orbital analysis. Excess electron density on N1 is also confirmed from ELF analysis. Further, the proton affinity (PA) and complex dissociation energy with

various Lewis acids (D_e (LA)), along with nucleophilicity indices (N), can be used to quantify the characteristics of these divalent N(I) systems.^{23–28}

3.3.1. Molecular Orbital and ELF Analyses. Molecular orbital (MO) analysis (Figure 4) of TTP1, TIP1, and TOP1

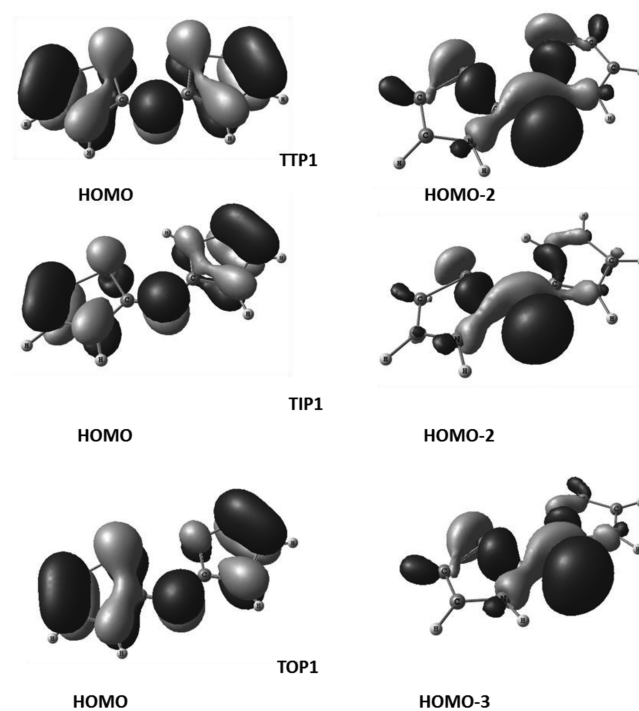


Figure 4. MO contour plots.

shows the two highest occupied MO orbitals correspond to π -type HOMO and σ -type (HOMO-2/HOMO-3) lone-pair orbitals with a maximum coefficient of electron density at the central nitrogen atom. The orbital occupancies at N1 are listed in Table 3. NBO analysis of these systems shows two lone pairs of electrons on the central nitrogen occupying σ and π orbital (Table 3). These are considerably larger than the electron occupancies in the σ and π lone pairs in carbones (1.51 and 1.11, respectively)¹⁰ but similar to the reported divalent N(I) systems,^{25,28} indicating that the lone pairs are strongly localized on the central nitrogen in these systems. Further, ELF analysis also indicates the greater localization of electron density at N1 in TIP1, TTP1, and TOP1 systems with $V(N1) > 3.00$ e, much larger than 2.00 e, which is expected for simple imine (Table 3). Contour plots (Figure S9, Supporting Information) generated through ELF analysis clearly show a bean-shaped isosurface at N1 displaying an excess electron localization in TTP1, TIP1, and TOP1.

Table 3. Comparison of NBO Charges, Nucleophilicity Parameters, and ELF Values of TTP1, TIP1, and TOP1 Complexes with Established ($L \rightarrow N \leftarrow L$)⁺ System (I)

	q_N^a	N^b	$N_k^-^c$	f_k^-	ELF ^a	$LP_{(N1)\sigma}^a$	$LP_{(N1)\pi}^a$
I	-0.745	1.43	0.512	0.358	3.32	1.78	1.56
TTP1	-0.721	1.35	0.429	0.317	3.13	1.84	1.47
TIP1	-0.724	1.45	0.474	0.327	3.20	1.82	1.50
TOP1	-0.726	1.37	0.434	0.317	3.17	1.82	1.49

^aValues are given in electrons. ^bGlobal nucleophilicity index is given in eV. Enforced NBO used for locating two lone pairs. ^cLocal nucleophilicity values for N1 center (the N_k^- values for other nitrogen centers are provided in Table S2, Supporting Information). Enforced NBO used for locating two lone pairs.

The estimated nucleophilicity indices (global (N) and local (N_k^- at N1)) of these systems at the B3LYP/6-311+G(d,p) level are found to be in the range ($N = 1.35$ – 1.45 , $N_k^- = 0.429$ – 0.474) (Table 3) reported for divalent N(I) systems.^{27,28} The estimated lower values of global nucleophilicity (N) and comparatively higher values of local nucleophilicity indices (N_k^-) at the N1 atomic center in comparison to N3, N8, and N11 (only in case of TIP1) centers (Table S2, Supporting Information) in these compounds are in accordance with the cationic nature of divalent N(I) systems.

3.3.2. Study of Proton Affinity and Lewis Base Character.

The compounds with divalent N(I) nitrogen are known to show mild nucleophilicities; this was attributed to the overall positive charge on these systems which resist proton attack to some extent. However, these species may help in proton exchanges in body fluid while remaining mildly active.^{23,25,87} The relative strength of nucleophilicity in these systems can be estimated in terms of proton affinity and complex dissociation energies with various Lewis acids. Table 4 lists the gas- and solvent-phase PAs for the three systems TTP1, TIP1, and TOP1, and the corresponding 3D optimized geometries are provided in Figures S10–S12 of the Supporting Information. The gas-phase PA value for TTP1 is 118.6 kcal/mol, for TIP1 it is slightly larger (124.3 kcal/mol), and for TOP1 it is slightly smaller (115.2 kcal/mol) (Table 4). These values are within the range of PA reported (~ 108 – 128 kcal/mol) for divalent N(I) species.^{23–28} Thus, with an increase in the dielectric constant of the medium the PA values are observed to increase (up to 25 kcal/mol) for divalent N(I) systems. The system TIP1 shows maximum PA of 149.6 kcal/mol in aqueous media. This study indicates that divalent N(I) compounds TTP1, TIP1 and TOP1 are rather safe for biological applications due to their mild basicity and under physiological conditions, they show a sufficient increase in the basicity which facilitates proton exchange in body fluids while remaining mildly active.

The mild nucleophilicity indices of divalent N(I) systems (TTP1, TIP1, and TOP1) are also reflected in their binding potential with various Lewis acids. The values for D_e (BH_3) are 13.6, 14.1, and 13.8 kcal/mol, respectively (Table 4), for TTP1, TIP1, and TOP1 systems, which are in accordance with the reported values.^{25,27} In terms of energy values, the polar solvent conditions slightly improve the strength of dissociation by 2–4 kcal/mol. The proton affinity values and complex dissociation energy (D_e (BH_3), D_e ($AlCl_3$), D_e ($AuCl$), and D_e ($AuCl$)₂) values indicate that TTP1, TIP1, and TOP1 indeed possess ($L \rightarrow N \leftarrow L$)⁺ character, and this character is more pronounced in the polar solvents. Thus, under physiological conditions, the distinctive expression of this hitherto novel bonding character in the protonated state of TT, TI, and TO systems is expected.

3.3.3. Rationalizing the Nucleophilicity Trend. The proton affinity of these three ($L \rightarrow N \leftarrow L$)⁺ systems follow the order

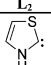
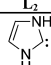
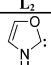
Table 4. Comparison of Proton Affinity (PA)^{a,b} Values, and Complex Dissociation Energy D_e ^{a,b} (with BH_3 , $AlCl_3$, and $AuCl$ ^c) of TTP1, TIP1, and TOP1 Systems in Gas- and Different Solvent-Phase Conditions

	TTP1	TIP1	TOP1
PA (H ⁺)			
gas	118.6	124.3	115.2
THF	140.8	146.4	139.1
DCM	141.4	147.0	139.7
ethanol	143.3	148.6	141.8
water	144.1	149.6	142.6
D_e (BH_3)			
gas	13.6	14.1	13.8
THF	15.8	17.5	16.5
DCM	15.8	17.6	16.5
ethanol	16.1	17.9	16.8
water	15.8	18.2	17.0
D_e ($AlCl_3$)			
gas	13.5	15.7	14.5
THF	13.0	23.8	18.1
DCM	13.1	24.1	18.2
ethanol	13.5	24.5	18.7
water	13.6	25.2	18.9
D_e ($AuCl$)			
gas	22.3	23.1	22.4
THF	23.5	25.5	24.0
DCM	23.5	25.6	24.1
ethanol	23.6	25.9	24.2
water	23.7	26.0	24.3
D_e ($AuCl$) ₂			
gas	<i>d</i>	31.4	27.1
THF	29.6	36.7	30.4
DCM	29.7	36.8	30.5
ethanol	30.1	37.6	31.1
water	30.3	37.9	31.3

^aValues given in kcal/mol. ^bPAs and complex dissociation energies (D_e) of compounds were calculated at B3LYP/6-311+G(d,p) level. ^cCalculations were carried out using mixed basis set approach (6-311+G(d,p) plus def2-TZVPP). ^dGeometry optimization of complex with two AuCl ligands did not lead to energy minima.

TIP1 > TTP1 > TOP1. However, the nucleophilicity trend is in the order TIP1 > TOP1 > TTP1. This change in the trend can be explained on the basis of suggestion given by Gusev, according to which the σ donating capacity of ligand L depends on electronic as well as steric parameters; this is clearly evident even in small NHC ligands.⁷⁶ The electronic as well as steric parameters of three ligands were analyzed on the NHC \rightarrow Ni(CO)₃ complexes (Table 5, Figure S15; Supporting Information). It is revealed from the data that nucleophilicity values of TTP1, TIP1, and TOP1 (Table 4) follow the trends

Table 5. Comparison of Electronic and Steric Descriptors of N-, S-, and O-Based Heteroazol-2-ylidenes

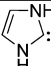
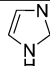
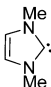
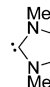
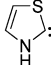
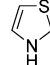
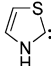
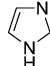
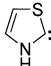
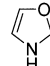
	L ₂ 	L ₂ 	L ₂ 
Nature of NHCs	Push-Push	Push-Push	Push-Push
$\nu_{\text{CO}}(\text{Al})\text{-Ni}(\text{CO})_3^a$	2123	2119	2127
TEP	2110	2107	2113
r-repulsiveness	0.53	0.00	0.21
ΔH elimination ^{b,c}	18.9	20.3	19.4
V_{min}^b	-69.02	-78.72	-69.84
$D_e(\text{BH}_3)\text{-L}^b$	45.2	49.0	45.7

^aA₁-symmetrical CO stretching frequency with values in cm⁻¹. ^bIn kcal/mol. ^cElectronic energies were taken into consideration. TEP reported in cm⁻¹. NOTE: TEP calculations were carried out using the equation given in Figure S17, and the MESP isosurface is represented in Figure S16 (Supporting Information).

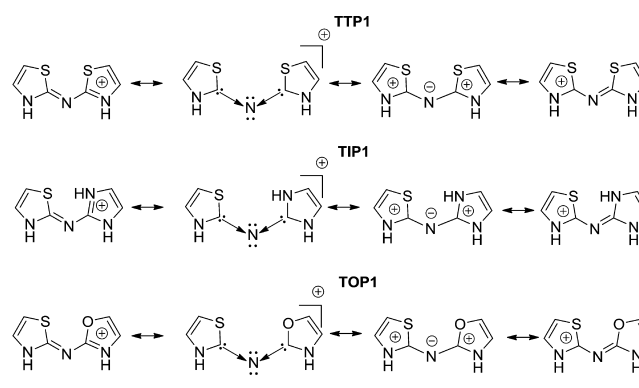
emerging from the steric descriptor (*r*) but not limited to the electronic descriptor (TEP). The reaction enthalpy (ΔH) for CO elimination from NHC → Ni(CO)₃ complex, V_{min} and $D_e(\text{BH}_3)\text{-L}$ values also correlate well with the steric descriptor. This comparative study establishes the hypothesis that the nucleophilicity of divalent N(I) compounds also need to be analyzed in terms of electronic as well as a steric descriptor of coordinating ligand (L). Our results are also supported by the recent study reported by Kelemen et al. on the investigation of the effect of heteroatoms (N, O, S, Se) on the stability of NHCs.⁸⁸

3.3.4. L → N Bond Strength analysis. As per the discussions in the previous section, the L → N bonds in **TTP1**, **TIP1**, and **TOP1** can be treated as coordinate bonds. However, valencies at C and N centers will be satisfied when the bonds are considered as π bonds also. Hence, it is important to establish the C → N character unambiguously. If there is strong π character across C–N bonds in these three systems, they should have linear structures (R₂C=N=CR₂)⁺ as in allenes, with orthogonal π bonds,²⁶ but the bent shape of these three systems clearly rules out this possibility. If there is any classical π character across the C–N bonds, the rotational barriers across the C–N bonds should be >30 kcal/mol.⁸⁹ The C–N bond rotational barrier in **I** is 2.8 kcal/mol,²⁵ which increased marginally to 3.6 kcal/mol in **TIP1**, which pointed out the fact that these bonds are not regular π bonds. In the case of (oxazol-2-ylidene) → N and (thiazol-2-ylidene) → N interactions in **TOP1** and **TTP1**, rotational barriers are again found to be low (7.2 and 9.5 kcal/mol) (Table 6), which directly indicate the uncertainty of π bonds in these systems. The work of Nyulaszi and co-workers^{90,91} reported the low rotational barriers for, the C–P bond rotation in imidazolium phosphonide⁹¹ zwitterions (**V**, Figure S18, Supporting Information) and established the inversely polarized ylidic character in them. Considering this argument, the C–N bonds in **TTP1**, **TIP1**, and **TOP1** may be considered to carry zwitterionic (charge-separated) character as represented by resonance form III (L⁺–N[–]–L⁺) in Scheme 3. The result from the Nyulaszi and co-workers⁹¹ state that the extent of delocalization within the imidazolium ring in ylidic compounds is found to be reduced in comparison to corresponding systems with imidazol-2-ylidene unit. As a result, we calculated the Bird index (BI), along with global nucleophilicity (*N*), electrodonating power (ω^-), and ELF values for compound **V** at MP2(full)/6-311+G(d,p) level. The results are presented in Table S5 of Supporting Information. It is clearly evident from the analysis that the BI for the imidazolium ring of compound **V** is found to be 57 which is

Table 6. Bond Dissociation Energies D_e (kcal/mol) and Energies with Inclusion of Thermal and Vibration Corrections D_0^{298} (kcal/mol) Calculated at the MP2(full)/6-311+G(d,p) Level

Entry	L ₁	L ₂	D_e	D_0^{298}	Rotational barrier	
					N1-C2	N1-C7
I			371.7	366.3	2.8 ^a	2.8 ^a
I-Me			379.6 ^b	--	-- ^c	-- ^c
TTP1			374.7	370.2	7.2	7.2
TIP1			373.8	368.5	8.5	3.6
TOP1			375.1	370.00	7.8	9.5
(N←C(NH ₂) ₂) ₂ ⁺	(NH ₂) ₂ C:	(NH ₂) ₂ C:	386.7	380.0	3.8 ^a	3.8 ^a
(N←N ₂) ₂ ⁺	N ₂	N ₂	96.2 ^b	94.1 ^b	-- ^c	-- ^c

^aValues are taken from ref 25. ^bValues are taken from ref 35. ^cCalculation of rotational barriers did not lead to energy minima.

Scheme 3. Schematic Representation of the Resonance Forms of **TTP1**, **TIP1**, and **TOP1** Isomers

lower in comparison to basic imidazol-2-ylidene moiety (BI = 62), while in **TIP1**, this value is found to be exactly similar for imidazolium unit, which suggests that this unit is indeed imidazol-2-ylidene in **TIP1**. Similarly, the values of BI for oxazolium ring in **TOP1** is found to be almost comparable to that of their corresponding carbene counterpart. However, the BI values for thiazolium rings in **TTP1** and **TOP1** systems show an increase delocalization (BI = 59 and 60) in comparison to free thiazol-2-ylidene (BI = 55) species. Similar, observation

is also noticed experimentally by Arduengo et al.⁹² for bis(carbene)-M complexes where M = Cu, Ag. Further, Frenking et al.⁹³ also report the related studies where they made computational estimation of this perception. Hence, the related literature on this conception also supports our proposition. Furthermore, the ELF values also show considerable differences in the population of electrons at N1 ($V(N1) = 3.13\text{--}3.20$ e in **TTP1**, **TIP1**, and **TOP1**) and at P ($V(P) = 1.81$ e in **V**) center. The above results confirm the excess electron localization at central nitrogen in these compounds, which is also observed qualitatively in plots of electron density difference provided in Figure S23, of Supporting Information. These results suggest that the notation with arrows ($L \rightarrow N \leftarrow L$)⁺ as represented in resonance form II (Scheme 3) can be strongly supported among the possible resonance representations.

Further, the analysis of donor–acceptor bond strength in these systems is also an important aspect of the discussion. Frenking et al.³⁵ suggested a method for estimating the bond dissociation energies (BDEs) of nitrogen-based cationic complexes with various ligands. They carried out the comparative analysis to study the dissociation energies of ($L \rightarrow N \leftarrow L$)⁺ complexes with various ligands, which revealed that BDE is larger for ($\text{NHC} \rightarrow N \leftarrow \text{NHC}$)⁺ (**I-Me**) ($D_e = 379.6$ kcal/mol) complex.³⁵ Along the similar lines, we have carried out BDEs analysis by using the equation ($L_1 \rightarrow N \leftarrow L_2$)⁺ $\rightarrow N^+(X^3P) + L_1 + L_2$. Table 6 shows the data for BDEs which are estimated at MP2(full)/6-311+G(d,p) level of approximation. The results revealed that bond dissociation energies of **TTP1**, **TIP1**, and **TOP1** complexes lie in the range of 373–375 kcal/mol (Table 6), which is comparable to that of BDEs reported by Frenking et al. for ($\text{NHC} \rightarrow N \leftarrow \text{NHC}$)⁺ complex. Further, these values are also in comparison to that of BDEs of **I** ($D_e = 371.7$ kcal/mol) indicating the existence of coordination bonds ($L \rightarrow N$) in **TTP1**, **TIP1**, and **TOP1** systems. The higher values of BDEs for divalent N(I) complexes also suggest that $L \rightarrow N$ interaction is stronger in these systems due to cationic nature of acceptor moiety. Among **TTP1**, **TIP1**, and **TOP1** systems, the highest value for BDE is observed in **TOP1**. In a compound **TOP1**, ligands bound more strongly with nitrogen cation in comparison to **TTP1** and **TIP1**. It can be the effect of oxazol-2-ylidene which forms a strong bond with central nitrogen owing to its higher π backdonation ($L \leftarrow N$) capability as compared to thiazol-2-ylidene and imidazol-2-ylidene ligands, this is also supported by the value of C–N rotational barriers which is highest for oxazol-2-ylidene $\rightarrow N$ bond in **TOP1**.

Taken together, the results reported in this section on **TTP1**, **TIP1**, and **TOP1** systems indicate that these species have an excessive partial negative charge, higher N_k^- values, localized population basin, and two lone pairs of π and σ symmetry, at N1 along with low $L \rightarrow N$ rotational barriers. Taking these factors into account, these species can be considered to carry divalent N(I) character with ($L \rightarrow N \leftarrow L$)⁺ electronic structure,^{23–29} which may exist as a hybrid of resonating structures shown in Scheme 3.

3.4. Molecular Docking Analysis. To demonstrate the importance of the ionic state and correct tautomeric representation of **TZA** derivatives during molecular docking studies, the docking analysis of aminic and iminic forms of **TT** and **TI** derivatives in their physiological states (protonated) was performed with the enzyme Lck (a member of the Src family of nonreceptor protein tyrosine kinases), which is expressed

mainly in T-lymphocytes. Compounds with promising Lck inhibitory activity found their use in T-cell-mediated disorders.⁹⁴ Zhu et al.⁸² reported the crystal structure for Lck kinase bound with non-hydrolyzable ATP mimic ANP, which shows that the important molecular recognition interactions are Ser323, Met319, and Glu317 key amino acid residues in the active site. Das et al.⁵⁰ reported a series of novel benzothiazole-based small molecules as potent inhibitors of Lck. Out of the series of reported ligands, BMS-358233 (2-aminopyrimidinyl) and BMS-350751 (2-aminopyridyl) were found to be highly potent Lck inhibitors in *in vitro* studies. The proposed molecular recognition interactions of BMS-358233 with Lck involve hydrogen bonds with Met319, Glu320, and Tyr318. Some of the ligands in this series are structural derivatives of **TT** and **TI** systems (i.e., **1** and **2**, Figure 5), which were

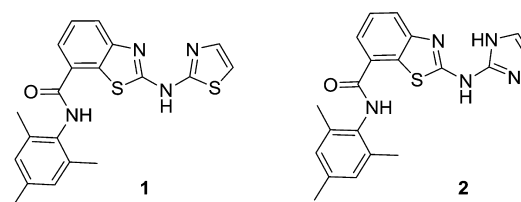


Figure 5. **TT**- and **TI**-substituted ligands used for docking analysis.

selected for carrying out molecular docking analysis (Figure S20, Supporting Information). Docking studies were carried out using the Glide module of Maestro 9.3.5 in the Schrödinger package. In order to reproduce the reported binding interaction, validation of docking protocol was performed with BMS-358233 on the domain of Lck kinase. BMS-358233 was able to reproduce the reported H bonding interactions with key amino acid residues (Figure 6a) with the docking score of $G_{\text{score}} = -6.71$. Later, compounds **1** and **2** in their protonated aminic (**1_a⁺** and **2_a⁺**) and iminic (**1_i⁺** and **2_i⁺**) tautomeric forms were docked in the active site, and it was found that the iminic (**1_i⁺**) form would be capable of showing H-bonding interactions with the key amino acid residues (Met319, Glu320, Tyr318, Figure 6b) as shown by BMS-325833, with a G_{score} of -6.80 . Similarly, the iminic (**2_i⁺**) form of compound **2** also binds in the cavity in a fashion similar to that of **1_i⁺** and forms H-bonding with Met319, Glu320, and Tyr318 through ring nitrogens ($G_{\text{score}} = -5.70$). The aminic forms **1_a⁺** and **2_a⁺** do not show the desired interactions and exhibit low docking scores (Figure S21 and Table S9, Supporting Information). The docking poses of these two compounds (**1** and **2**) clearly show that two distinct tautomeric forms possess different pharmacophoric features and choosing a correct tautomeric representation plays a significant role in identifying the drug receptor interactions. The central nitrogen atoms in **1_i⁺** and **2_i⁺** are in their divalent N(I) state; this study helps in analyzing that drug action in such class of compounds involve divalent N(I) state, and thus, this character plays an important role in molecular recognition of drugs carrying bis(azole)amine group.

4. CONCLUSIONS

Quantum chemical calculations using the DFT (B3LYP, ω B97X-D) method were carried out to solve the structural dichotomy associated with bis(azole)amine analogues. A study on the isomeric preferences (in the gas phase and implicit/explicit solvation models) clarifies that the title compounds

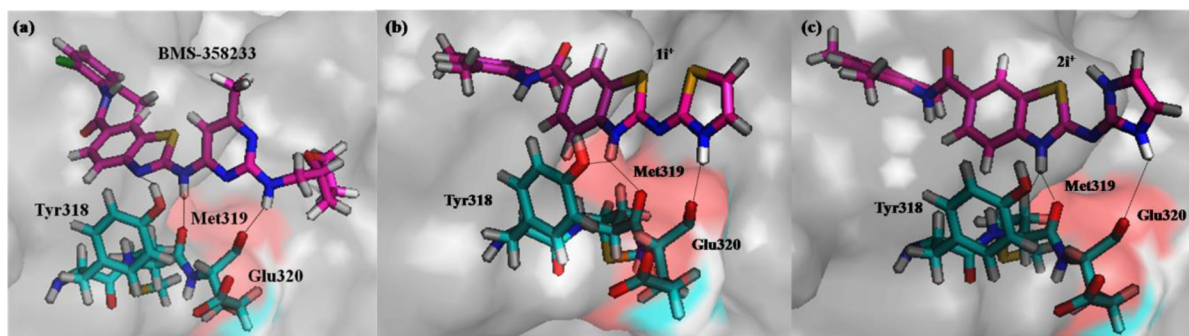


Figure 6. Docked pose and H-bonding interactions of (a) BMS-358233 (potent inhibitor of Lck) and iminic forms (b) $1i^+$ and (c) $2i^+$ in the active site of lymphocyte-specific kinase Lck (PDB-ID: 1QPC). Dashed lines show H-bonding interactions.

should be treated as the derivatives of thiazol-2-imine rather than thiazol-2-amine. The stability of iminic forms (global minimum tautomers) can be rationalized in terms of (i) 4π -electron conjugation, and (ii) $N3\cdots H12\cdots N8$ intramolecular hydrogen bond.

Since the bis(azole)amines prefer to exist in an iminic state, **TT**, **TI**, and **TO** can be treated as $L \rightarrow N-R$ compounds with hidden divalent $N(I)$ character, in which L is an electron-donating heterazol-2-ylidene. They are highly basic (large protonation energy), and upon protonation, these species prefer to exist in a tautomeric state defined by $(L \rightarrow N \leftarrow L)^+$ arrangement, where L is heterazol-2-ylidene (N -heterocyclic carbene). In these divalent $N(I)$ compounds, the central nitrogen carries (i) a formal positive charge and (ii) two lone pairs of electron (σ and π -type), which is evident by the localization of electron density, and (iii) low $L \rightarrow N$ rotational barrier.

Cationic divalent $N(I)$ species show low proton affinities (~ 115 – 124 kcal/mol). However, the polarity of the solvent medium influences the proton affinity as well as nucleophilicity of these species. The role of differential ligating properties of heterazol-2-ylidene in the stabilization of the central coordinating nitrogen was systematically explored. The **TIP1** (thiazol-2-ylidene $\rightarrow N \leftarrow$ imidazol-2-ylidene) $^+$ system is characterized by moderate nucleophilic character with the maximum localization of electron density at the central nitrogen atom. The complex dissociation energies (D_e) of the (**TOP1**) (thiazol-2-ylidene)-(oxazol-2-ylidene) $N^+ \rightarrow M$ ($M = BH_3, AlCl_3, AuCl$) system are found to be better than that of (**TTP1**) ((thiazol-2-ylidene) $_2N^+ \rightarrow M$, which in turn reflects the better coordination strength of the former species. These studies suggest that the steric factor of coordinating ligands “ L ”, also plays a significant role (in addition to electronic factors) in metal coordination of $(L \rightarrow N \leftarrow L)^+$ systems. Molecular docking studies of substituted thiazol-2-amine derivatives with Lck kinase domain were also performed in order to demonstrate the importance of cationic and imine tautomeric representation for this class of compounds. This study helps in establishing the novel electronic structure of the therapeutic lead compounds, belonging to bis(azole)amine class and help in understanding their drug action.

■ ASSOCIATED CONTENT

📄 Supporting Information

2D figures of medicinally relevant N -substituted thiazole-2-amine derivatives and molecular graphs from AIM calculations. 3D-optimized geometries and coordinates of compounds discussed in the text at the B3LYP/6-311+G(d,p) level of

theory. Contour plots for **TTP1**, **TIP1**, and **TOP1** systems. Plots of HOMOs to visualize the localization of π type lone pairs in dicationic species. Glide scores and docking poses for ANP and cationic aminic states of **1** and **2**. This material is available free of charge via the Internet at <http://pubs.acs.org>.

■ AUTHOR INFORMATION

Corresponding Author

*Tel: +91-172-2292018. Fax: +91-172-2214692. E-mail: pvbharatam@nipер.ac.in.

Notes

The authors declare no competing financial interest.

■ ACKNOWLEDGMENTS

S.B. acknowledges financial support received from the INSPIRE division of Department of Science and Technology (DST), New Delhi, India. We are thankful to the reviewers of this article for their valuable suggestions.

■ REFERENCES

- (1) Dyker, C. A.; Bertrand, G. *Nat. Chem.* **2009**, *1*, 265–266.
- (2) Alcarazo, M.; Lehmann, C.; Anoop, A.; Thiel, W.; Fürstner, A. *Nat. Chem.* **2009**, *1*, 295–301.
- (3) Frenking, G.; Tonner, R. In *Contemporary Carbene Chemistry*; John Wiley & Sons, Inc.: New York, 2013; pp 216–236.
- (4) Deshmukh, M. M.; Gadre, S. R.; Tonner, R.; Frenking, G. *Phys. Chem. Chem. Phys.* **2008**, *10*, 2298–2301.
- (5) Frenking, G.; Tonner, R. *Pure Appl. Chem.* **2009**, *81*, 597–614.
- (6) Guha, A. K.; Phukan, A. K. *Chem.—Eur. J.* **2012**, *18*, 4419–4425.
- (7) Patel, D. S.; Bharatam, P. V. *Curr. Sci.* **2010**, *99*, 425–426.
- (8) Phukan, A. K.; Guha, A. K. *Dalton Trans.* **2012**, *41*, 8973–8981.
- (9) Tonner, R.; Frenking, G. *Angew. Chem., Int. Ed.* **2007**, *46*, 8695–8698.
- (10) Tonner, R.; Frenking, G. *Chem.—Eur. J.* **2008**, *14*, 3260–3272.
- (11) Tonner, R.; Frenking, G. *Chem.—Eur. J.* **2008**, *14*, 3273–3289.
- (12) Tonner, R.; Heydenrych, G.; Frenking, G. *Chem. Phys. Chem.* **2008**, *9*, 1474–1481.
- (13) Tonner, R.; Öxler, F.; Neumüller, B.; Petz, W.; Frenking, G. *Angew. Chem., Int. Ed.* **2006**, *45*, 8038–8042.
- (14) Parameswaran, P.; Frenking, G. *Chem.—Eur. J.* **2009**, *15*, 8807–8816.
- (15) Takagi, N.; Tonner, R.; Frenking, G. *Chem.—Eur. J.* **2012**, *18*, 1772–1780.
- (16) Takagi, N.; Shimizu, T.; Frenking, G. *Chem.—Eur. J.* **2009**, *15*, 3448–3456.
- (17) Takagi, N.; Shimizu, T.; Frenking, G. *Chem.—Eur. J.* **2009**, *15*, 8593–8604.
- (18) Mondal, K. C.; Samuel, P. P.; Tretiakov, M.; Singh, A. P.; Roesky, H. W.; Stückl, A. C.; Niepötter, B.; Carl, E.; Wolf, H.; Herbst-Irmer, R. *Inorg. Chem.* **2013**, *52*, 4736–4743.

- (19) Sidiropoulos, A.; Jones, C.; Stasch, A.; Klein, S.; Frenking, G. *Angew. Chem., Int. Ed.* **2009**, *48*, 9701–9704.
- (20) Bruns, H.; Patil, M.; Carreras, J.; Vázquez, A.; Thiel, W.; Goddard, R.; Alcarazo, M. *Angew. Chem., Int. Ed.* **2010**, *49*, 3680–3683.
- (21) Holzmann, N.; Dange, D.; Jones, C.; Frenking, G. *Angew. Chem., Int. Ed.* **2013**, *52*, 3004–3008.
- (22) Kunetskiy, R. A.; Cisarová, I.; Saman, D.; Lyapkalov, I. M. *Chem.—Eur. J.* **2009**, *15*, 9477–9485.
- (23) Patel, D. S.; Bharatam, P. V. *Chem. Commun.* **2009**, 1064–1066.
- (24) Mehdi, A.; Adane, L.; Patel, D. S.; Bharatam, P. V. *J. Comput. Chem.* **2010**, *31*, 1259–1267.
- (25) Patel, D. S.; Bharatam, P. V. *J. Phys. Chem. A* **2011**, *115*, 7645–7655.
- (26) Patel, D. S.; Bharatam, P. V. *J. Org. Chem.* **2011**, *76*, 2558–2567.
- (27) Bhatia, S.; Bagul, C.; Kasetti, Y.; Patel, D. S.; Bharatam, P. V. *J. Phys. Chem. A* **2012**, *116*, 9071–9079.
- (28) Bhatia, S.; Malkhede, Y. J.; Bharatam, P. V. *J. Comput. Chem.* **2013**, *34*, 1577–1588.
- (29) Kozma, A.; Gopakumar, G.; Farès, C.; Thiel, W.; Alcarazo, M. *Chem.—Eur. J.* **2013**, *19*, 3542–3546.
- (30) Wang, Y.; Xie, Y.; Wei, P.; King, R. B.; Schaefer, H. F., III; Schleyer, P. v. R.; Robinson, G. H. *J. Am. Chem. Soc.* **2008**, *130*, 14970–14971.
- (31) Wang, Y.; Xie, Y.; Wei, P.; Schaefer, H. F., III; Schleyer, P. v. R.; Robinson, G. H. *J. Am. Chem. Soc.* **2013**, *135*, 19139–19142.
- (32) Ellis, B. D.; Dyker, C. A.; Decken, A.; Macdonald, C. L. B. *Chem. Commun.* **2005**, 1965–1967.
- (33) Alcarazo, M.; Radkowski, K.; Mehler, G.; Goddard, R.; Furstner, A. *Chem. Commun.* **2013**, 49, 3140–3142.
- (34) Kinjo, R.; Donnadiou, B.; Celik, M. A.; Frenking, G.; Bertrand, G. *Science* **2011**, *333*, 610–613.
- (35) Celik, M. A.; Sure, R.; Klein, S.; Kinjo, R.; Bertrand, G.; Frenking, G. *Chem.—Eur. J.* **2012**, *18*, 5676–5692.
- (36) De, S.; Parameswaran, P. *Dalton Trans.* **2013**, 42, 4650–4656.
- (37) Abraham, M. Y.; Wang, Y.; Xie, Y.; Gilliard, R. J., Jr.; Wei, P.; Vaccaro, B. J.; Johnson, M. K.; Schaefer, H. F., III; Schleyer, P. v. R.; Robinson, G. H. *J. Am. Chem. Soc.* **2013**, *135*, 2486–2488.
- (38) Abraham, M. Y.; Wang, Y.; Xie, Y.; Wei, P.; Schaefer, H. F., III; Schleyer, P. v. R.; Robinson, G. H. *Chem.—Eur. J.* **2010**, *16*, 432–435.
- (39) Himmel, D.; Krossing, I.; Schnepf, A. *Angew. Chem., Int. Ed.* **2014**, *53*, 370–374.
- (40) Frenking, G. *Angew. Chem., Int. Ed.* **2014**, DOI: 10.1002/anie.201311022.
- (41) Ball, P. *Chemistry World*, February 2014, 11, 50–54
- (42) Shaik, S.; Danovich, D.; Wu, W.; Hiberty, P. C. *Nat. Chem.* **2009**, *1*, 443–449.
- (43) Shaik, S.; Danovich, D.; Silvi, B.; Lauvergnot, D. L.; Hiberty, P. C. *Chem.—Eur. J.* **2005**, *11*, 6358–6371.
- (44) Alvarez, S.; Hoffmann, R.; Mealli, C. *Chem.—Eur. J.* **2009**, *15*, 8358–8373.
- (45) Schreiner, P. R.; Chernish, L. V.; Gunchenko, P. A.; Tikhonchuk, E. Y.; Hausmann, H.; Serafin, M.; Schlecht, S.; Dahl, J. E. P.; Carlson, R. M. K.; Fokin, A. A. *Nature* **2011**, *477*, 308–311.
- (46) Bader, R. F. W. *J. Phys. Chem. A* **2010**, *114*, 7431–7444.
- (47) Hollóczki, O.; Kelemen, Z.; Nyulászi, L. *J. Org. Chem.* **2010**, *77*, 6014–6022.
- (48) Zhong, M.; Bui, M.; Shen, W.; Baskaran, S.; Allen, D. A.; Elling, R. A.; Flanagan, W. M.; Fung, A. D.; Hanan, E. J.; Harris, S. O. *Bioorg. Med. Chem. Lett.* **2009**, *19*, 5158–5161.
- (49) Kumbhare, R. M.; Dadmal, T.; Kosurkar, U.; Sridhar, V.; Rao, J. V. *Bioorg. Med. Chem. Lett.* **2012**, *22*, 453–455.
- (50) Das, J.; Moquin, R. V.; Lin, J.; Liu, C.; Doweyko, A. M.; DeFex, H. F.; Fang, Q.; Pang, S.; Pitt, S.; Shen, D. R. *Bioorg. Med. Chem. Lett.* **2003**, *13*, 2587–2590.
- (51) Geronikaki, A.; Eleftheriou, P.; Vicini, P.; Alam, I.; Dixit, A.; Saxena, A. K. *J. Med. Chem.* **2008**, *51*, 5221–5228.
- (52) Geronikaki, A. A.; Lagunin, A. A.; Hadjipavlou-Litina, D. I.; Eleftheriou, P. T.; Filimonov, D. A.; Poroikov, V. V.; Alam, I.; Saxena, A. K. *J. Med. Chem.* **2008**, *51*, 1601–1609.
- (53) Eleftheriou, P.; Geronikaki, A.; Hadjipavlou-Litina, D.; Vicini, P.; Filz, O.; Filimonov, D.; Poroikov, V.; Chaudhaery, S. S.; Roy, K. K.; Saxena, A. K. *Eur. J. Med. Chem.* **2012**, *47*, 111–124.
- (54) Vicini, P.; Geronikaki, A.; Incerti, M.; Zani, F.; Dearden, J.; Hewitt, M. *Bioorg. Med. Chem. Lett.* **2008**, *16*, 3714–3724.
- (55) Deshmukh, R.; Thakur, A. S.; Jha, A. K.; Deshmukh, R. *Int. J. Res. Pharm. Chem.* **2011**, *1*, 229–333.
- (56) Grassi, A.; Ippen, J.; Bruno, M.; Thomas, G. *Eur. J. Pharmacol.* **1991**, *195*, 251–259.
- (57) Téllez, F.; Peña-Hueso, A.; Barba-Behrens, N.; Contreras, R.; Flores-Parra, A. *Polyhedron* **2006**, *25*, 2363–2374.
- (58) Cruz, A.; Gayosso, M.; Contreras, R. *Heteroatom Chem.* **2001**, *12*, 586–593.
- (59) Matisova-Rychla, L.; Rychly, J.; Meske, M.; Schulz, M. *Polym. Degrad. Stab.* **1988**, *21*, 323–333.
- (60) Mohamed, A. A.; El-Harby, A. W. *THEOCHEM* **2007**, 817, 125–136.
- (61) Boedecker, J.; Pries, H.; Roesch, D.; Malewski, G. *J. Prakt. Chem.* **1975**, *317*, 953–958.
- (62) Parr, R. G.; Yang, W. *Density-Functional Theory of Atoms and Molecules*; Oxford University Press: New York, 1989.
- (63) Becke, A. J. *Chem. Phys.* **1993**, *98*, 5648–5652.
- (64) Lee, C.; Yang, W.; Parr, R. *Phys. Rev. B* **1988**, *37*, 785–789.
- (65) Chai, J.-D.; Head-Gordon, M. *Chem. Phys.* **2008**, *10*, 6615–6620.
- (66) Frisch, M. J.; Trucks, G. W.; Schlegel, H. B.; Scuseria, G. E.; Robb, M. A.; Cheeseman, J. R.; Scalmani, G.; Barone, V.; Mennucci, B.; Petersson, G. A. *Gaussian 09: EM64L-G09 Rev. B.01*, Gaussian, Inc., Wallingford, CT, 2010. (For the full reference, see the Supporting Information).
- (67) Scott, A. P.; Radom, L. *J. Phys. Chem.* **1996**, *100*, 16502–16513.
- (68) Barone, V.; Cossi, M. *J. Phys. Chem. A* **1998**, *102*, 1995–2001.
- (69) Reed, A. E.; Curtiss, L. A.; Weinhold, F. *Chem. Rev.* **1988**, *88*, 899–926.
- (70) Biegler-König, F.; Schönbohm, J.; Bayles, D. J. *Comput. Chem.* **2001**, *22*, 545–559.
- (71) Becke, A. D.; Edgecombe, K. E. *J. Chem. Phys.* **1990**, *92*, 5397.
- (72) Lu, T.; Chen, F. *J. Comput. Chem.* **2012**, *33*, 580–592.
- (73) Traeger, J. C. *J. Phys. Chem. A* **2008**, *112*, 342–346.
- (74) Maksic, Z. B.; Kovacevic, B. *J. Org. Chem.* **2000**, *65*, 3303–3309.
- (75) Weigend, F.; Ahlrichs, R. *Phys. Chem. Chem. Phys.* **2005**, *7*, 3297–3305.
- (76) Gusev, D. G. *Organometallics* **2009**, *28*, 6458–6461.
- (77) Mathew, J.; Suresh, C. H. *Inorg. Chem.* **2010**, *49*, 4665–4669.
- (78) Domingo, L. R.; Chamorro, E.; Pérez, P. *J. Org. Chem.* **2008**, *73*, 4615–4624.
- (79) Gazquez, J.; Cedillo, A.; Vela, A. *J. Phys. Chem. A* **2007**, *111*, 1966–1970.
- (80) Chattaraj, P. K.; Maiti, B. *J. Phys. Chem. A* **2001**, *105*, 169–183.
- (81) Pratihari, S.; Roy, S. *J. Org. Chem.* **2010**, *75*, 4957–4963.
- (82) Zhu, X.; Kim, J. L.; Newcomb, J. R.; Rose, P. E.; Stover, D. R.; Toledo, L. M.; Zhao, H.; Morgenstern, K. A. *Structure* **1999**, *7*, 651–661.
- (83) Sastry, G. M.; Adzhigirey, M.; Day, T.; Annabhimoju, R.; Sherman, W. *J. Comput. Aided Mol. Des.* **2013**, *27*, 221–234.
- (84) Friesner, R. A.; Banks, J. L.; Murphy, R. B.; Halgren, T. A.; Klicic, J. J.; Mainz, D. T.; Repasky, M. P.; Knoll, E. H.; Shelley, M.; Perry, J. K. *J. Med. Chem.* **2004**, *47*, 1739–1749.
- (85) *LigPrep, Suite 5*, Schrödinger, LLC, New York, 2012.
- (86) Lemau de Talence, V.; Hissler, M.; Zhang, L.-Z.; Karpati, T.; Nyulászi, L.; Caras-Quintero, D.; Bauerle, P.; Reau, R. *Chem. Commun.* **2008**, 2200–2202.
- (87) Bharatam, P.; Patel, D.; Iqbal, P. *J. Med. Chem.* **2005**, *48*, 7615–7622.
- (88) Kelemen, Z.; Holloczki, O.; Olah, J.; Nyulászi, L. *RSC Adv.* **2013**, *3*, 7970–7978.

- (89) Kumar, R. S.; Marwaha, A.; Bharatam, P. V.; Mahajan, M. P. *THEOCHEM* **2003**, *640*, 1–12.
- (90) Nyulaszi, L.; Veszpremi, T.; Reffy, J. *J. Phys. Chem.* **1995**, *99*, 10142–10146.
- (91) Majhi, P. K.; Schnakenburg, G.; Kelemen, Z.; Nyulaszi, L.; Gates, D. P.; Streubel, R. *Angew. Chem., Int. Ed.* **2013**, *52*, 10080–10083.
- (92) Arduengo, A. J., III; Dias, H. V. R.; Calabrese, J. C.; Davidson, F. *Organometallics* **1993**, *12*, 3405–3409.
- (93) Frenking, G.; Sola, M.; Vyboishchikov, S. F. *J. Organomet. Chem.* **2005**, *690*, 6178–6204.
- (94) Hanke, J. H.; Pollok, B. A.; Changelian, P. S. *Inflammation Res.* **1995**, *44*, 357–371.